JOURNAL OF MATERIALS SCIENCE **36** (2001) 4755–4762

Effect of yttrium on high temperature oxidation behavior of Ni-Al-Mo-B alloy IC6

C. B. XIAO, Y. F. HAN
Beijing Institute of Aeronautical Materials (BIAM), P.O. Box 81-1, Beijing 100095, People's Republic of China
E-mail: CBXiao@263.net

A variety of experimental techniques have been used to study the effect of yttrium on the high temperature cyclic oxidation behavior of a directionally solidified (DS) Ni-Al-Mo-B alloy IC6. The cyclic oxidation resistance of alloy IC6 is substantially improved by adding proper amount of yttrium, which is resulted from several beneficial roles played by yttrium. Yttrium decreases the harmful effect of sulfur to the adherence between the oxides scale and the substrate, and the depth of the diffusion layer by inhibiting cationic transportation. Yttrium promotes the selective oxidation of aluminum and decreases the proportion of NiO region in the surface oxide scale. Yttrium migrates to the oxide grain boundaries and promotes the formation of a fine close packed oxide grain structure, and hence improves the mechanical strength of the grain boundaries.

1. Introduction

One of the critical requirements for a protective oxide scale on an alloy substrate to provide high temperature environmental resistance is that the scale should be adherent to the substrate. It is well known that one of the best ways to improve the adherence of oxide scales, notably Cr_2O_3 and Al_2O_3, is adding small amount of a rare earth element, as a component in the alloy. Various explanations have been proposed to account for the beneficial effects of active element addition. These include: (a) inhibition of segregation of sulfur to the interface between oxide scale and substrate [1–10]; (b) enhancement of scale plasticity by modifying the structure [11–22]; (c) reduction in accumulation of voids at the alloy/scale interface [23–27]; (d) mechanical keying by the formation of oxide pegs [11, 13, 23, 28–35]; (e) reduction of growth stress through the modification to growth process of the oxide scale [14, 15, 20, 21, 36–41].

A directionally solidified (DS) alloy IC6 has been recently developed in BIAM as a high-temperature structural material used for advanced jet-engine blades and vanes operating in the temperature range of 1050–1150°C [42]. Its high temperature oxidation resistance is substantially improved by adding proper amount of yttrium [43, 44], the purpose of this paper is to investigate the beneficial roles played by yttrium.

2. Experimental procedure

The master alloy with the chemical composition of Ni—(7.5–8.5)Al—(13.0–15.0)Mo—(0.02–0.1) B (wt%) was first prepared by a vacuum induction furnace, and then the columnar grain specimens with addition of different amount of yttrium were produced by rapid solidification technique in a commercial DS vacuum induction furnace. The as-cast specimens were homogenized at 1260°C for 10 h and oil quenched.

The specimens with the size of $30 \times 10 \times 1.5$ mm were oxidized in air at 1100°C in furnace to let the oxidation scale form and spall naturally and taken out after different length of time to weigh the mass change with analytical balance.

The specimens after exposure at high temperature for X-ray line scan of elements were polished and then examined in a JXA 8600 electron probe microanalyzer (EPMA). The morphology of surface oxides was studied with JSM-35 type scanning electron microscope (SEM). The contents of spalled surface oxides were analyzed with MXP-AHF18 type X-ray diffraction instrument.

3. Results and discussion

3.1. Microstructure of alloy IC6 with and without yttrium

The microstructure of alloy IC6 after homogenization was examined by SEM. The results showed that the microstructure of alloy IC6 can be divided into interdendritic and dendritic areas, A and B respectively, as shown in Fig. 1. The dark phase is γ' phase and the gray phase in network is γ phase. The volume percent of γ phase is about 20–25% and that of γ' phase is about 75–80%. The dimension of γ' precipitates is 0.1–0.3 μm in interdendritic area and 1–3 μm in dendritic area. Boride usually appears in the interdendritic area when boron content exceeds 0.16 at% [45].

The chemical composition analysis results showed that the actual level of yttrium was about 20–25% of the nominally added amount. The result of SEM showed

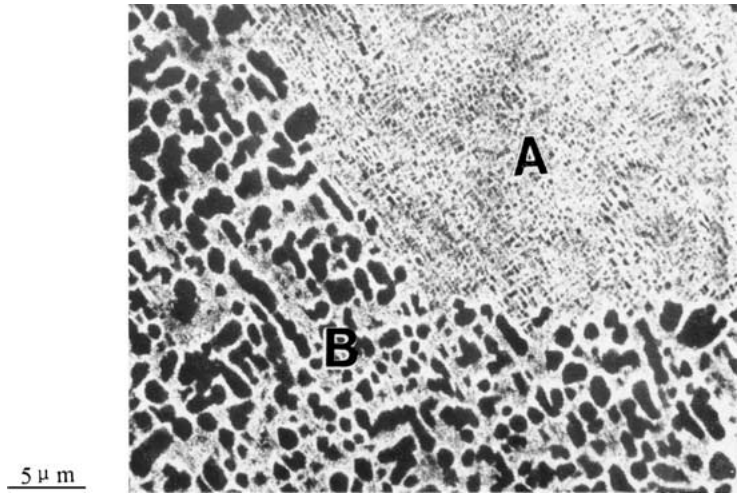

Figure 1 SEM image of alloy IC6 showing the interdendritic area A and dendritic area B.

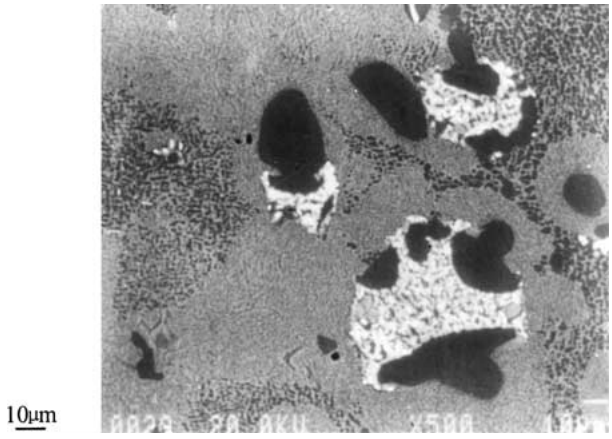

Figure 2 Back scattered electron image (BSEI) of alloy with 0.20–0.30 wt% Y showing the bulk shape regions.

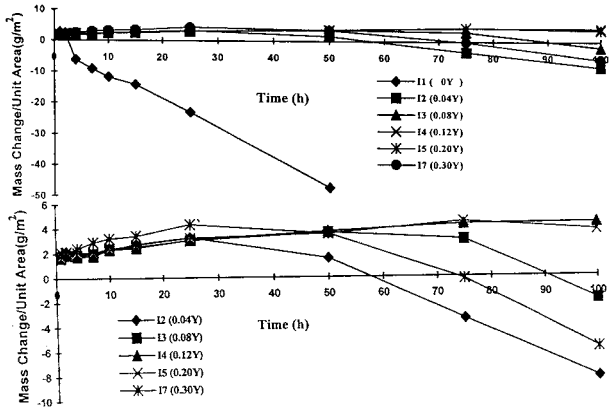

Figure 3 The mass change per unit area *vs* time at 1100°C. (a). for all heats, (b). details of (a) for heats I2, I3, I4, I5, I7.

that the microstructure of alloy IC6 with addition of 0.04–0.12 wt% yttrium has no obvious difference compared with that of alloy without yttrium. When the added amount of yttrium increases to 0.20 wt%, bulk shape regions is formed in the interdendritic area surrounded by large size γ' precipitates, as shown in Fig. 2. The volume percent of bulk shape region and large size γ' precipitates in the interdendritic area increases when the amount of yttrium increases from 0.2 wt% to 0.3 wt%. The conventional TEM and EDS analysis results show that the bulk shape regions consist of three phases, one of them is γ phase, the other containing only Ni and Y was identified to be Ni_3Y, and the third one containing only Mo and Ni was identified to be $Mo_{1.24}Ni_{0.76}$ [46].

3.2. Oxidation test results

Cyclic oxidation test was carried out at 1100°C in air. Three samples of each heat were tested at the same time and taken out of the furnace to determine the mass change. The average mass change per unit area of three samples of each heat *vs* time is plotted in Fig. 3. From Fig. 3a, it can be seen that the scale of alloy IC6 without yttrium (I1) spalls severely after about 2 h. For analysis convenience, the point that mass change becomes minus value is defined as the beginning time for severe scale spallation (BTSSS). BTSSS of alloys with yttrium is obviously longer than that of alloy without yttrium. The details of several heats in Fig. 3a have been shown in Fig. 3b. From Fig. 3b it can be seen that the severe scale spallation time of I2 (adding 0.04 wt% Y) starts at about 58 h and that of I3 (adding 0.08 wt% Y) starts at about 90 h, and no severe spallation of scale in I4 (adding 0.12 wt% Y) and I5 (adding 0.20 wt% Y) is found within 100 h. While the mass change in I5 (adding 0.20 wt% Y) started decreasing after 75 h very slightly, and the BTSSS is about at 73 h when the adding amount of yttrium increases to 0.3 wt% (I7). It can be concluded that the adherence of scale to the substrate of alloy IC6 is substantially improved by adding proper amount of yttrium.

The results of cyclic oxidation tests of several alloys which were carried out at 1100°C in ONERA, France are shown in Fig. 4, where alloy IC6 ONERA was produced according to the optimum nominally chemical composition and alloy IC6 ONERA mod is the modified alloy IC6 ONERA with addition of the micro-alloying elements Si and Hf, and both alloys were produced in ONERA. The chemical compositions of the alloys in Fig. 4 are given in Table I. From Fig. 4 it can be seen that the cyclic oxidation resistance of alloy IC6 with addition of proper amount of yttrium (0.12 wt%) is much better than that of alloy IC6 and even better than that of alloy DS Mar-M200 with addition of hafnium.

TABLE I Chemical composition of alloys (wt%)

Alloy	C	Cr	Co	Al	Ti	Mo	W	Nb	Hf	Si	Y	Zr	B	Ni
IC6+Y	–	–	–	7.51	–	13.95	–	–	–	–	0.026 0.12[a]	–	0.025	Bal.
IC6-ONERA	–	–	–	7.64	–	13.6	–	–	–	–	–	–	0.022	Bal.
IC6-ONERA mod	–	–	–	7.64	–	13.6	–	–	0.098	0.101	–	–	0.022	Bal.
DS 200 Hf[b]	0.15	9.0	10.0	5.0	2.0	–	12.5	1.0	2.0	–	–	0.05	0.015	Bal.

[a]added amount.
[b]nominal composition for alloy DS 200 Hf.

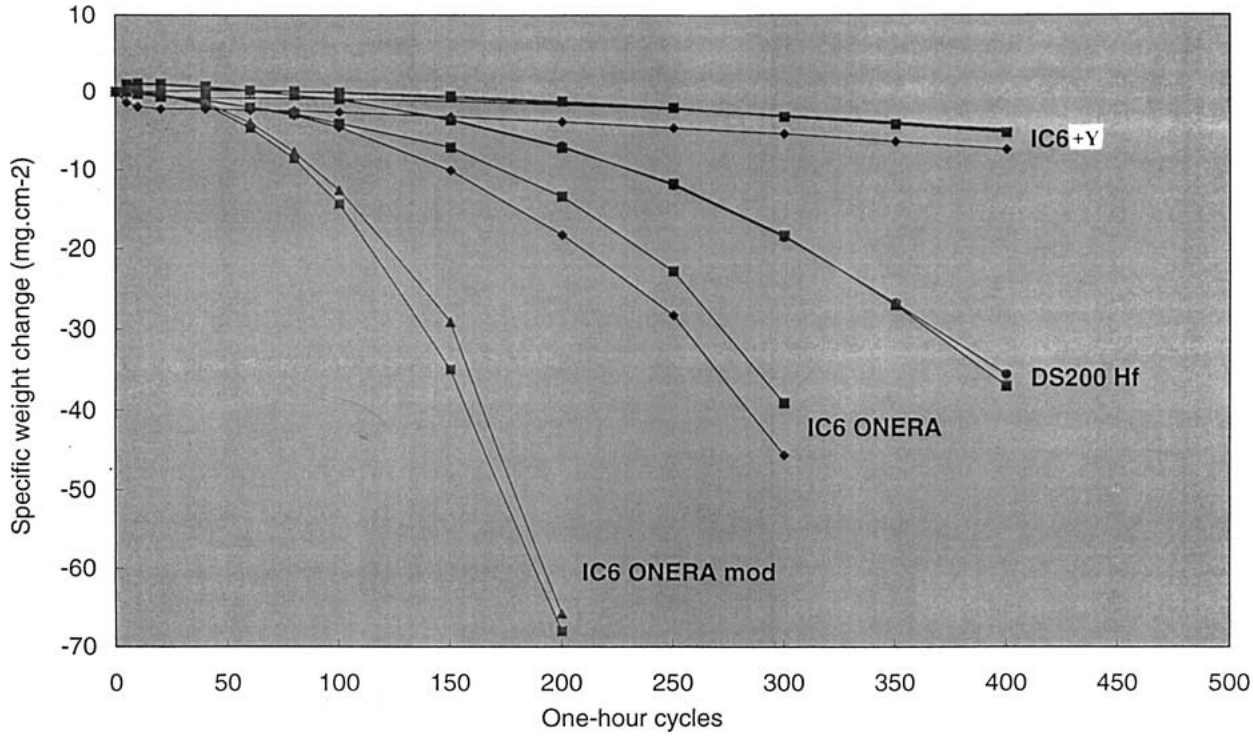

Figure 4 Cyclic oxidation test results of several alloys in air at 1100°C.

However, adding Si and Hf simultaneously to alloy IC6 has no beneficial effect to its cyclic oxidation resistance unlike alloy B-1900, Mar-M200 and In 713C [47].

3.3. Beneficial effects of yttrium in improving oxidation resistance

The reasons of improvement of the high temperature isothermal and cyclic oxidation resistance of alloy IC6 by adding yttrium were analyzed using the scanning electron microscopy, x-ray line scan for elements of EPMA and X-ray diffraction technique. The beneficial roles of yttrium on high temperature oxidation resistance to be stated respectively include: (a) decreasing the harmful effect of sulfur to the adhesion of oxide scale to the substrate; (b) decreasing the depth of the diffusion layer; (c) promoting the selective oxidation of aluminum; (d) decreasing the proportion of easily spalled NiO region in the surface oxide scale and promoting the formation of a fine close packed oxide grain structure; (e) migrating to the oxide grain boundaries and improving the mechanical strength of the grain boundaries, changing the oxide scale spallation cracks of the yttrium modified alloy from intergranular to be transgranular. The decrement of oxidation resistance for the alloy with addition of excess amount of yttrium may be attributed to the inner oxidation of Ni_3Y precipitated in the interdendritic area [46].

3.3.1. Decreasing the harmful effect of sulfur to the adhesion of oxide scale to the substrate

As been mentioned above, the adherence of oxide scale to the substrate of alloy IC6 can be substantially improved by adding proper amount of yttrium, which has been mainly attributed to the role of yttrium in decreasing the weakening role of sulfur to interface bond between oxide scale and substrate. Yttrium can easily react with sulfur to form sulfides of high incipient melting temperature during melting. The usual form of sulfide is Y_2S_3. The density of Y_2S_3 is 3.87 g/cm^3, which is much lower than that of alloy IC6 (7.90 g/cm^3). Y_2S_3 is floatable in the melt and can adhere to the wall of the crucible during melting. Hence the content of sulfur remained in the alloy is decreased. Generally, the

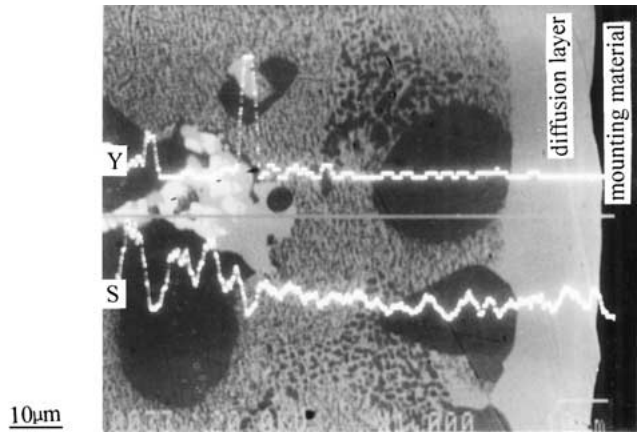

Figure 5 X-ray line scan showing the trapping role to sulfur played by the phases rich in yttrium during high temperature oxidation process.

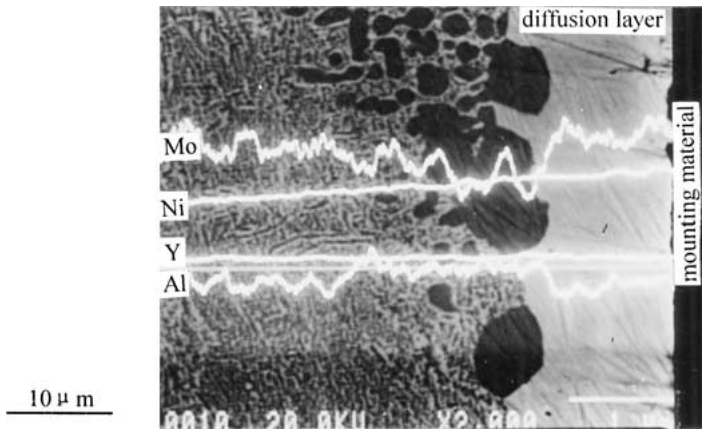

Figure 6 Diffusion layer formed in the specimens after exposure at 1100°C, and the X-ray line scan for Mo, Ni, Y, Al.

amount of sulfur is about 10 ppm in alloy IC6 without yttrium and 4–6 ppm in the alloys with addition of proper amount of yttrium. On the other hand, the bulk shape regions containing Ni_3Y mentioned in part 3.1 can act as traps to sulfur during high temperature oxidation process, as shown in Fig. 5. The amount of sulfur which segregates to oxide scale/substrate interface and weakens the interface bond is reduced due to the above two roles played by yttrium.

3.3.2. Decreasing the depth of diffusion layer

There is no consecutive oxide scale formed in the surface of specimens after exposure at 1100°C in air. A diffusion layer is formed in the surface or beneath the oxide scale of all heats studied, as shown in Fig. 6. From the X-ray line scan for elements results in Fig. 6, it can be seen that the diffusion layer is rich in Mo and Ni, while poor in Al. A large amount of Ni_3Mo with $D0_{22}$ type crystal structure is formed in the diffusion layer due to the enrichment of Mo and Ni [48].

The diffusion layer is primarily a function of Al consumed to form oxides. The wider the diffusion layer, the more spallation of oxides scale. More spallation means more Al consumption as oxides try to reform. The presentation of yttrium can inhibit the cationic transportation and hence affect the depth of diffusion layer formed in the specimens after exposure at 1100°C, as shown in Fig. 7. The depth of diffusion layer of alloy IC6 without

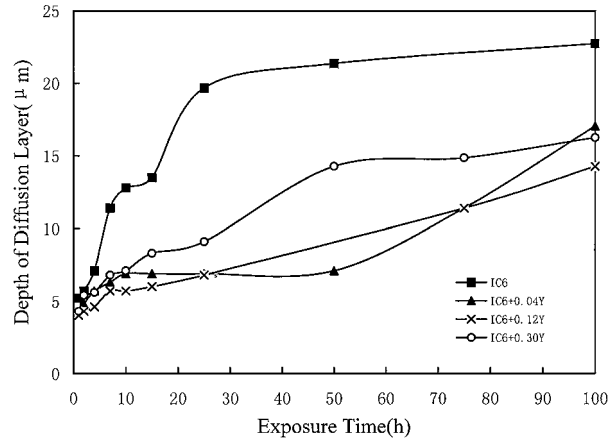

Figure 7 Effect of yttrium on the depth of diffusion layer.

yttrium increases very quickly before 25 h and reaches nearly 23 μm after exposure at 1100°C for 100 h. For the alloy with addition of 0.04 wt% Y, the depth of diffusion layer increases slowly before 50 h but accelerates after 50 h and is up to 17 μm after 100 h. The depth increases very slowly and evenly all through 100 h to reach 14 μm for the alloy with addition of 0.12 wt% Y. When the adding amount of yttrium increases to 0.30 wt%, though the depth of diffusion layer increases very slowly during 50–100 h, the increment of the depth of diffusion layer is only a little slower than that of alloy without yttrium before 50 h, and hence it exceeds 16 μm after exposure at 1100°C for 100 h.

3.3.3. Promoting selective oxidation of aluminum

The oxide scale spalled severely of alloy IC6 without yttrium during cyclic oxidation. As been mentioned above, the adherence of oxide scale to the substrate is substantially improved for the alloys with addition of proper amount of yttrium. The amount of spalled oxide scale decreases with the increasing addition amount of yttrium in the range of 0.04–0.12 wt%, but increases when the addition amount of yttrium exceeds 0.20 wt%.

The X-ray diffraction results of spalled oxide scales formed during cyclic oxidation show that the spalled oxides are mainly consisted of NiO and $NiA1_2O_4$ for both alloys with and without yttrium [49], which indicates that NiO and $NiA1_2O_4$ spalled easily. The main difference in spalled oxides between alloys with and without yttrium is that there are some α–Al_2O_3 formed in the alloys with addition of yttrium [49], which indicates that yttrium can promote the selective oxidation of aluminium and hence improve the oxidation resistance of alloy IC6.

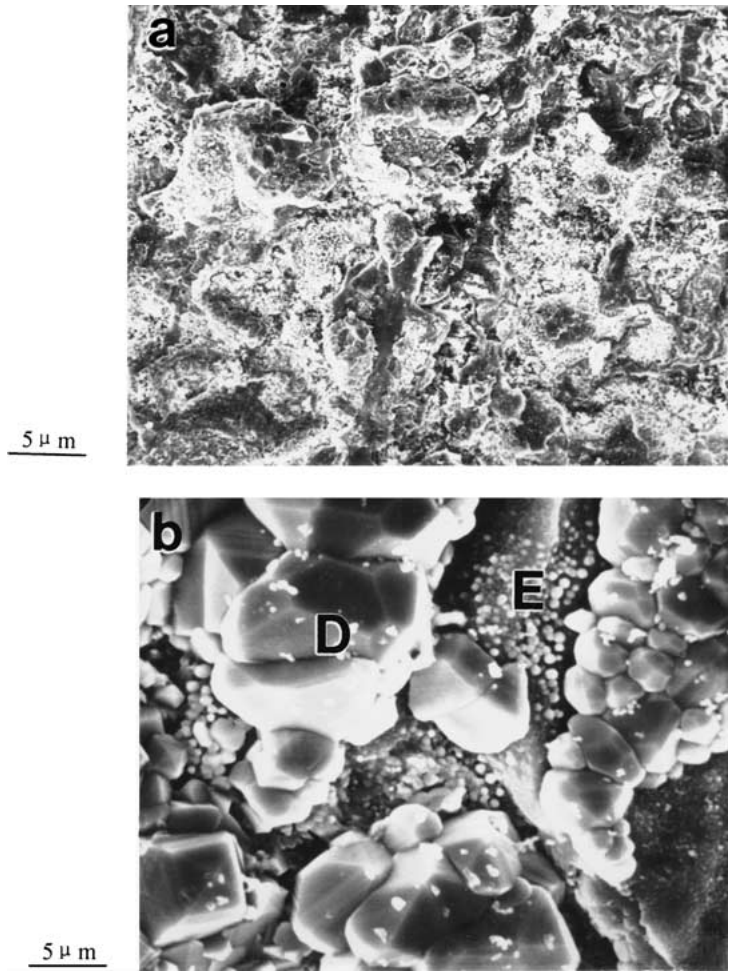

Figure 8 Surface oxide morphology of alloy IC6 without yttrium after exposure at 1100°C for 100 h. (a) Low magnification, (b) High magnification.

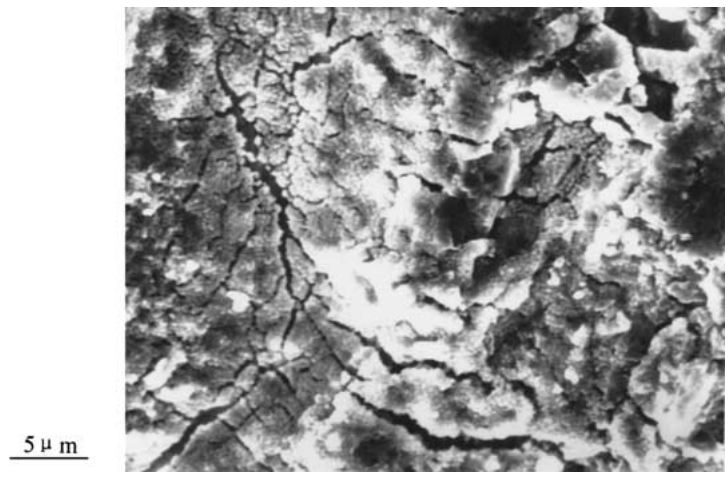

Figure 9 The cracks in most of region E of alloy IC6 without yttrium.

3.3.4. Decreasing the proportion of NiO region in surface oxide scale

The surface oxide scale formed in alloy IC6 with and without yttrium during high temperature oxidation can be divided into two regions according to the energy dispersive spectrum (EDS) analysis results, one region called region D is purely consisted of NiO, the other one called region E is consisted of other oxides mentioned in part (3.3.3) except NiO. Region D can be spalled much more easily than region E. Yttrium can decrease the proportion of region D and increase that of region E. The low and high magnification SEM images of surface oxide morphology of alloy IC6 without yttrium are illustrated in Fig. 8a and b respectively, from which it can be seen that the oxide scales are mainly consisted of region D with large grain size of NiO. Even in most of region E, there are many cracks, which indicate the poor strength between oxide grain boundaries, as shown in Fig. 9. For the alloys with addition of proper amount of yttrium, the proportion of region D in surface oxides decreases and that of region E increases, as shown in Fig. 10. From the high magnification image of region D and region E, it can be seen that the oxide grains in both regions are more fine and closely packed than that

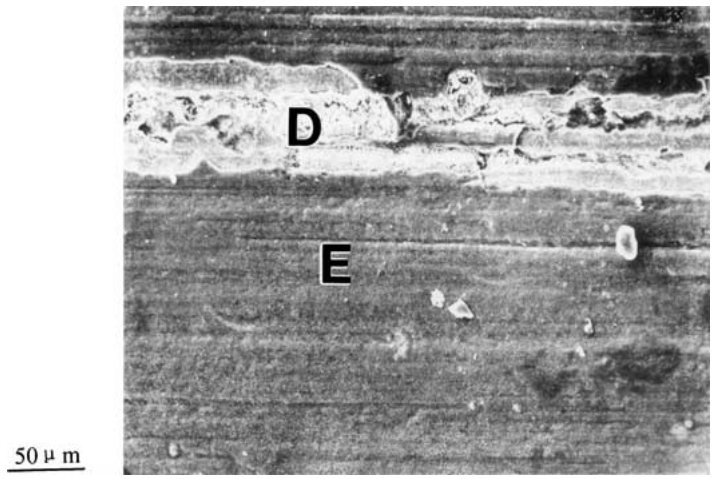

Figure 10 Surface oxide morphology of alloys with addition of yttrium after exposure at 1100°C for 100 h.

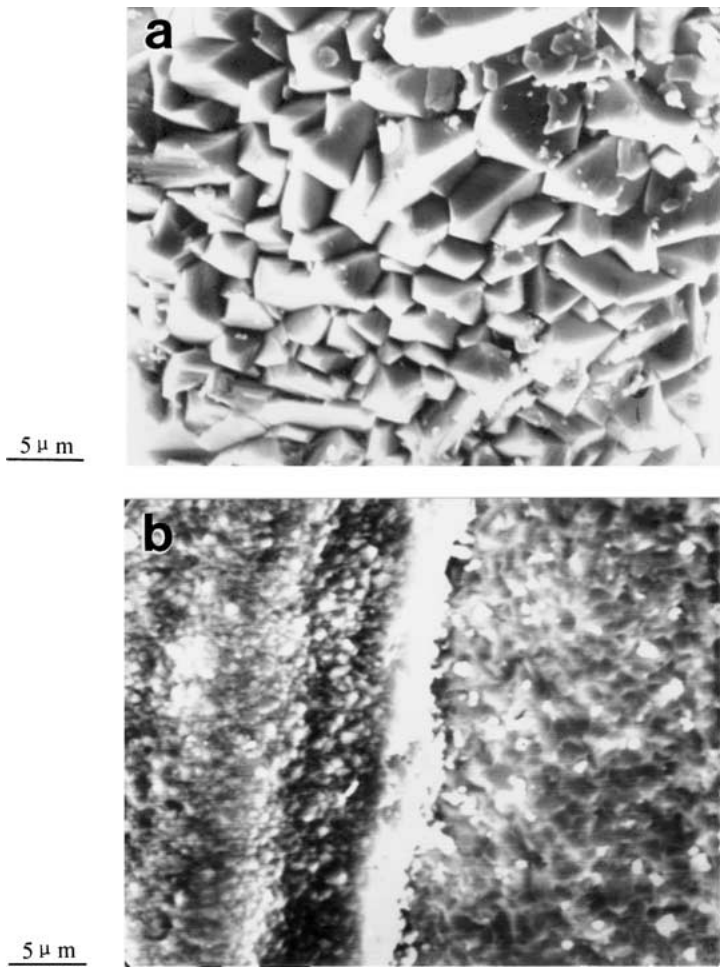

Figure 11 High magnification image of region D and region E in Fig. 10. (a) Region D, (b) Region E.

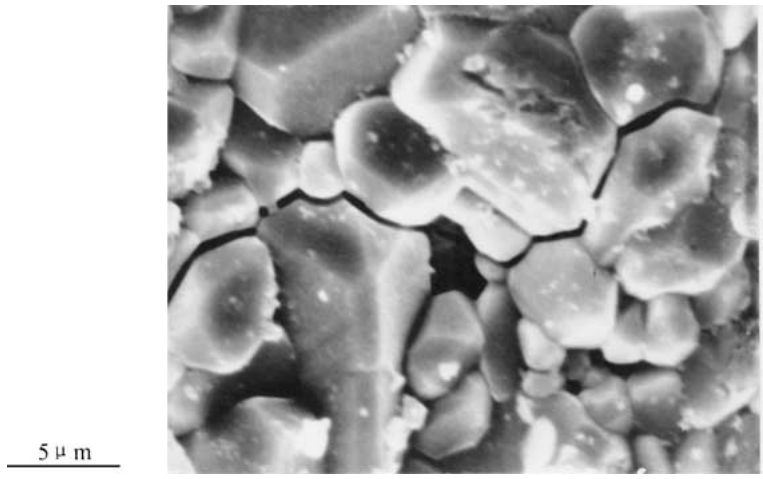

Figure 12 Spallation crack of NiO in alloy IC6 without yttrium.

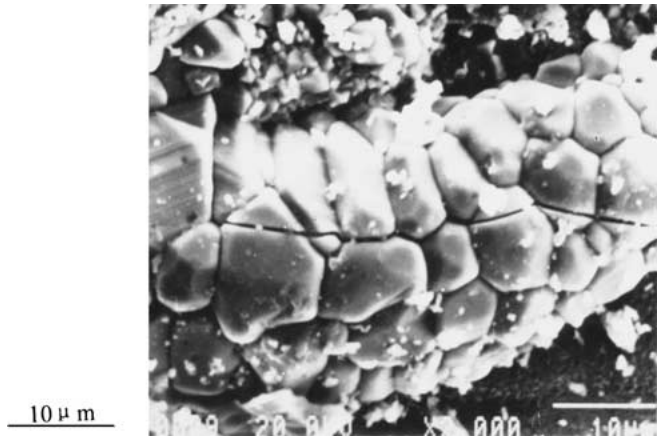

Figure 13 Spallation crack of NiO in alloy IC6 with addition of yttrium.

in alloys without yttrium, as shown in Fig. 11a and b respectively.

3.3.5. Migrating to oxide grain boundaries and improving mechanical strength of grain boundaries

The X-ray diffraction results show that the spalled oxides mainly consist of NiO for both alloys with and without yttrium after oxidized at 1100°C for 100 h [49]. The surface oxide morphology was then examined for these specimens. The results show that the spallation cracks of NiO are mainly intergranular for the alloy without yttrium, as shown in Fig. 12. However, the spallation cracks of NiO have become dominantly transgranular for the alloy with addition of proper amount yttrium, as shown in Fig. 13. The transformation of NiO spallation from intergranular to transgranular is mainly attributed to the strengthening of the bonding of oxide grain boundaries by yttrium. Tawancy *et al*. [17, 18] quantitatively investigated the segregation of yttrium to the grain boundaries of α–$A1_2O_3$. Their research results showed that yttrium restricted grain boundary movement and helped maintain a fine-grained structure. In a fine-grained oxide structure, the stresses caused by oxide growth can be relieved easily by diffusional plastic flow, and hence the plasticity and fracture toughness of the oxide scale are improved. The transformation of NiO spallation from intergranular to transgranular, as shown in Figs. 12 and 13, indicates that yttrium is beneficial to improving the plasticity and fracture toughness of NiO and preventing it from spalling.

4. Conclusions

The effect of yttrium on high temperature cyclic oxidation behavior of a Ni-Al-Mo-B alloy IC6 was investigated in the present study, the results show that the adherence of scale to the substrate of alloy IC6 is substantially improved by adding proper amount of yttrium.

The beneficial effects of yttrium on high temperature cyclic oxidation resistance of alloy IC6 include: (a) decreasing the harmful effect of sulfur to the adherence between oxide scale and substrate; (b) decreasing the depth of diffusion layer by inhibiting cationic transportation; (c) promoting the selective oxidation of aluminum; (d) decreasing the proportion of NiO region which is easy to be spalled in surface oxide scale; (e) migrating to the oxide grain boundaries and improving the mechanical strength of grain boundaries.

Acknowledgments

The authors wish to acknowledge the Advanced Materials Committee of China and SNECMA, France for

the financial supports, and Dr. P. Caron, who is with ONERA for his work on cyclic oxidation tests of the alloys.

References

1. A. W. FUNKENBUSCH, J. G. SMEGGIL and N. S. BORNSTEN, *Metall. Trans.* **16A** (1985) 1164.
2. J. G. SMEGGIL, A. W. FUNKENBUSCH and N. S. BORNSTEN, *ibid.* **17A** (1986) 923.
3. E. SCHUMANN, J. C. YANG and M. J. GRAHAM, *Scripta Materialia* **34** (1996) 1365.
4. M. W. BRUMM and H. J. GRABKE, *Corr. Sci.* **34** (1993) 547.
5. R. HUTCHINGS, M. H. LORETTO and R. E. SMALLMAN, *Metal Science* **15** (1981) 7.
6. H. J. GRABKE, D. WIEMER and H. VIEFHAUS, *Applied Surf. Sci.* **47** (1991) 243.
7. J. ALEXANDER, *Mater. Sci. & Tech.* **1** (1985) 167.
8. Y. IKEDA, M. TOSA and K. YOSHIHARA, *Mater. Sci. Eng.* **A 120** (1989) 179.
9. J. G. SMEGGIL, A. J. SHUSKUS, N. S. BORNSTEIN and M. A. DE CRESCENTE, in "The Role of Active Elements in the Oxidation Behaviour of High Temperature Metals and Alloys," edited by E. Lang (Elsevier Applied Science, London, 1989) p. 271.
10. JAMES L. SMIALEK, *Metall. Trans.* **18A** (1987) 164.
11. J. E. ANTILL and K. A. PEAKALL, *J. Iron Steel Inst.* **205** (1967) 1136.
12. J. M. FRANCIES and J. A. JUSTON, *Corros. Sci.* **6** (1968) 445.
13. J. K. TIEN and F. S. PETTIT, *Metall. Trans.* **3** (1972) 1587.
14. T. A. RAMANARAYANAN, M. RAGHAVAN and R. PETKOVIC-LUTON, *Oxid. Met.* **22** (1984) 83.
15. *Idem., J. Electrochem. Soc.* **131** (1984) 923.
16. T. A. RAMANARAYANAN, R. AYER, R. PETKOVIC-LUTON and D. P. LETA, *Oxid. Met.* **22** (1988) 83.
17. H. M. TAWANCY, *Metall. Trans.* **22A** (1991) 1463.
18. H. M. TAWANCY and N. SRIDHAR, *Oxid. Met.* **37** (1992) 143.
19. L. V. RAMANATHAN, *Cor. Sci.* **35** (1993) 871.
20. P. KOFSTAD, in "The Role of Active Elements in Oxidation Behaviour of Metals and Alloys," edited by E. Lang (Elsevier Applied Science, London/New York, 1989) p. 367.
21. A. M. HUNTZ, in "The Role of Active Elements in Oxidation Behaviour of Metals and Alloys," edited by E. Lang (Elsevier Applied Science, London/New York, 1989) p. 81.
22. H. HINDAM and D. P. WHITTLE, *Oxid. Met.* **18** (1982) 245.
23. C. S. GIGGINS, B. H. KEAR, F. S. PETIT and J. K. TIEN, *Metall. Trans.* **5** (1974) 1685.
24. J. E. McDONALD and J. E. EBERHART, *ibid.* **233** (1965) 512.
25. J. D. KUENZLEY and D. L. DOUGLASS, *Oxid. Met.* **8** (1974) 139.
26. J. STRINGER, *Metall. Rev.* **11** (1966) 113.
27. J. STRINGER, B. A. WILCOX and R. I. JAFFEE, *Oxid. Met.* **5** (1972) 11.
28. I. A. ALLAM, D. P. WHITTLE and J. STRINGER, *ibid.* **12** (1978) 35.
29. B. LUSTMANN, *Trans. Metall. Soc. AEME* **188** (1950) 995.
30. C. S. WUKUSICK and J. F. COLLINS, *Mater. Res. Stand.* **4** (1964) 637.
31. J. M. FRANCIS and W. H. WHITLOW, *Corros. Sci.* **5** (1965) 701.
32. A. U. SEYBOLT, *ibid.* **6** (1966) 263.
33. C. W. PRICE, I. G. WRIGHT and G. R. WALLWORK, *Metall. Trans.* **4** (1973) 2423.
34. I. A. KVERNES, *Oxid. Met.* **6** (1973) 45.
35. I. A. ALLAM, D. P. WHITTLE and J. STRINGER, *ibid.* **13** (1978) 381.
36. F. A. GOLIGHTLY, F. H. STOTT and G. C. WOOD, *ibid.* **10** (1976) 163.
37. G. C. WOOD and F. H. STOTT, in "High Temperature Corrosion," edited by R. A. RAPP (NACE-6, Houston, TX, 1983) p. 227.
38. F. H. STOTT, in "The Role of Active Elements in the Oxidation Behaviour of High Temperature Metals and Alloys," edited by E. Lang (Elsevier Applied Science, London, 1989) p. 3.
39. J. JEDLINSKI, in "The Role of Active Elements in the Oxidation Behaviour of High Temperature Metals and Alloys," edited by E. Lang (Elsevier Applied Science, London, 1989) p. 131.
40. K. P. R. REEDY, J. L. SMIALEK and A. R. COOPER, *Oxid. Met.* **17** (1982) 429.
41. B. A. PINT, J. R. MARTIN and L. W. HOBBS, *ibid.* **39** (1993) 167.
42. Y. F. HAN, Z. P. XING and M. C. CHATURVEDI, in "Structural Intermetallics," edited by M. V. NATHAL, R. DAROLIA, C. T. LIU, P. L. MARTIN, D. B. MIRACLE, R. WAGNER and M. YAMAGUCHI, The Second International Symposium on Structural Intermetallics, Seven Springs Mountain Resort, Champion, Pennsylvania, Sep. 21–25, 1997, TMS, USA (1997) p. 713.
43. C. B. XIAO and Y. F. HAN, *Acta Metallurgica Sinica* (English Letters) **11** (1998) 296.
44. C. B. XIAO and Y. F. HAN, *Transactions of Nonferrous Metals Society of China* **9 Suppl. 1** (1999) 335.
45. Y. F. HAN, Y. M. WANG and M. C. CHATURVEDI, *J. Mater. Eng. Perf.* **2** (1993) 589.
46. C. B. XIAO and Y. F. HAN, *Scripta Materialia* **41** (1999) 475.
47. R. V. MINER, *Metall. Trans.* **8A** (1997) 1949.
48. C. B. XIAO and Y. F. HAN, *Scripta Materialia* **41** (1999) 1217.
49. C. B. XIAO and Y. F. HAN, *Acta Metallurgica Sinica* (in Chinese) **34** (1998) 1158.

Received 22 May 2000
and accepted 31 May 2001